基于街道图像与深度学习的城市景观研究

USING STREET-LEVEL IMAGES AND DEEP LEARNING FOR URBAN LANDSCAPE STUDIES

https://doi.org/10.15302/J-LAF-20180203 收稿时间 RECEIVED DATE / 2018-03-20 中图分类号 / TU98, TP18 文献标识码 / A

李小江
麻省理工学院城市研究与规划系感知城市实验室博士后研究员

蔡洋
麻省理工学院城市研究与规划系感知城市实验室研究助理

卡洛 · 拉蒂
麻省理工学院城市研究与规划系教授，感知城市实验室主任

Xiaojiang LI
Postdoctoral Fellow of Senseable City Lab, Department of Urban Studies and Planning, Massachusetts Institute of Technology
Room 9-250, 77 Massachusetts Avenue, Cambridge, MA 02139, USA
xiaojian@mit.edu

Bill Yang CAI
Research Assistant of Senseable City Lab, Department of Urban Studies and Planning, Massachusetts Institute of Technology

Carlo RATTI
Professor of Department of Urban Studies and Planning, and Director of Senseable City Lab, Massachusetts Institute of Technology

摘要

城市街道不仅是人类活动的集聚地，也是居民与城市建成环境发生社会交互的主要界面。因此，加深对于城市街道景观的了解在城市研究工作中至关重要。街道图像获取性的大大提高为城市景观研究提供了新的机遇，也提高了街道景观研究与分析的准确性与多样性。本研究基于街道图像，呈现了新近研发的深度卷积神经网络在景观分析中的应用。利用经过训练的深度卷积神经网络模型，我们能够准确地从街道图像中识别出不同的城市特征。根据图像分割技术处理结果，我们进一步测算出了马萨诸塞州剑桥市的街道绿化空间分布情况，并对街谷开阔程度进行了量化分析。诸如上述人工智能与大规模采集的街道图像的结合，将为世界范围内的城市景观研究提供全新的视角。

关键词
卷积神经网络；城市街道；人工智能；机器学习；图像分割

ABSTRACT

Streets are a focal point of human activities and a major interface of the social interaction between urban dwellers and urban built environment. A better understanding of the urban landscapes along streets is thus important in urban studies. The increasing availability of street-level images provides new opportunities for urban landscape studies to study and analyze streetscapes at a fine level and from a different perspective. In this study, we presented an application of a recently developed Deep Convolutional Neural Network on landscape analysis based on street-level images. Different urban features were identified from street-level images accurately using a trained Deep Convolutional Neural Network model. Based on the image segmentation results, we further measured the spatial distribution of the street greenery and quantitatively analyzed the openness of street canyons in Cambridge, Massachusetts. The proposed combination of Artificial Intelligence and the massively collected street-level images provides a new sight for urban landscape studies for cities around the world.

KEY WORDS
Convolutional Neural Network; Urban Street; Artificial Intelligence; Machine Learning; Image Segmentation

1 引言

城市街道既是居民与城市建成环境发生社会交互的主要界面，也是人类活动的集聚地[1]。作为城市景观特征的重要代表，街道深刻反映并影响着人们的生活方式、身心健康与社会福祉[1]。而基于街道尺度对城市环境进行量化分析则有助于深入了解城市街道的功能。

街道绿地是街道景观中必不可少的组成部分，它们发挥着重要的生态系统功能。其不仅有利于提升人们对城市风貌的审美能力[2][3]，也可美化住宅区街道，创造良好的步行条件[4]，亦有助于促进病人术后康复[5][6]。

整理 王颖 **译** 刘姝 王颖
EDITED BY Ying WANG **TRANSLATED BY** Shu LIU Ying WANG

① 更多有关“场所脉动”项目的信息，可参见 http://pulse.media.mit.edu/。

① For more information of the Place Pulse project, please visit http://pulse.media.mit.edu/.

除街道绿地外，街谷的几何形态也影响着行人的日常体验——其开阔程度直接决定了太阳辐射的多少，进而影响街道中行人的热舒适程度[1][7]，这一点在炎热的夏季尤需重视。此外，围合程度过高的街谷亦容易给行人造成压迫感，进而影响人们对环境的感知[8][9]。

在当前的城市研究中，人们通过多种不同的方法来模拟、衡量城市环境，且获取数据的途径也愈加多样。其中包括已应用于城市绿地、城市形态和城市环境建模等研究中的数字城市模型与高空间分辨率遥感数据。但这两种工具却并非适用于所有研究：一方面，数字城市模型常过度简化城市环境，且易忽视城市中的自然景观；另一方面，俯视视角的遥感数据无法反映街景的立面效果——即人在地面上的体验与感受[10]。

而用于捕捉街道景观形态的街道图像有着与行人类似的视角，因而开辟了从地面角度进行精细化城市景观研究的新途径。因呈现了街道景观的真实形态，且促使人们产生对城市环境的直观感知，结合了公众众包评级与评分过程的街景地图已得到广泛应用[11][12]。随着人工智能的不断发展，我们可以更加准确地从街道图像中获取语义信息，这一过程的自动化程度亦显著提高。例如，“场所脉动”[①]项目即是基于谷歌街景地图，通过众包形式对街区的安全性、居民富裕程度和活力指数进行评级。利用收集而来的谷歌街景地图与标记信息可训练模型

1 Introduction

City streets are a major interface of the social interaction between urban dwellers and urban built environment and a focal point of human activities in urban areas[1]. Streets are also one of the most critical urban landscape features reflecting and effecting people's lifestyles and physical, mental, and social well-being[1]. Quantification of the physical environment at street-level would offer great utility to understand the performances of urban street functions.

As an important part of the landscape along streets, the street greenery performs critical ecosystem functions. It helps increase people's esthetic rating of urban scenes[2][3] and the attractiveness and walkability of residential streets[4]. The visibility of urban greenery could even increase the restorative potential of patients from surgery[5][6].

Other than the street greenery, the geometry of the street canyon would also influence the daily experience of pedestrians. The openness of a street canyon has a direct impact on the level of its solar radiation and consequently the thermal comfort experienced at the street level[1][7]. This effect is more important during hot summers. In addition, human perception of the environment may also be influenced because enclosed street canyons may give a feeling of oppression to the pedestrians[8][9].

A variety of methods and data sources have been used to model and measure the urban physical environment in urban studies. For example, digital city models and high spatial resolution remotely sensed data have been used in studies of street greenery, urban form, and urban environment modeling. However, these two types of tools are not available for all studies. The digital city models usually over-simplify the urban environment and neglect the urban natural landscapes. In addition, the overhead-view remotely sensed data cannot reflect the profile view of streetscapes experienced and felt by people on the ground[10].

Street-level images, which capture the appearance of the streetscape and have similar view angle with pedestrians, provide new opportunities for urban landscape studies at a very fine level from the ground perspective. Since street-level images represent the physical appearance of streetscapes and are directly connected with human perceptions of the urban environment, street-level images have been used to map human perception of environment through crowdsourcing ratings and scores from the general public[11][12]. The advancement in Artificial Intelligence (AI) makes it possible to derive semantic information from street-level images automatically and accurately. For example, the Place Pulse[①] project crowdsourced ratings of neighborhoods

进行机器学习，进而在街区中生成新的语义信息[12]。蒂姆尼特·盖布鲁等人曾提出通过收集大量带有地理标签的街道图像来估测美国不同选区的社会经济情况[13]。其通过谷歌街景地图识别在不同街区中停放车辆的品牌与车型，再利用这些信息进一步判断当地居民的政治偏好与经济状况。在谷歌街景地图时间轴功能的帮助下，尼吉尔·奈克等选取美国五大城市中的街区进行研究，以探讨其环境随时间而发生的变化[14]。由上述社会因素与街道景观形态变化之间的紧密联系可见，基于街道图像的研究方法可帮助预测未来街区改善的方向。

在本文所呈现的研究中，基于街景地图分析与近年来逐渐发展成熟的深度卷积神经网络（DCNN），我们对街道绿化空间分布情况及街谷围合度进行了测量。研究结果表明，可公开获取的全球普遍可用的谷歌街景数据与人工智能技术的结合，将大力助推城市研究的发展。

2 研究区域与数据集

在本项研究中，我们选取美国马萨诸塞州剑桥市作为研究区域。剑桥市紧邻波士顿市北部，与波士顿市区隔河相对。剑桥市是马萨诸塞州人口第五大城市，总人口约10.5万人。

on attributes such as safety, wealth, and liveliness based on Google Street View (GSV) images. Using collected GSV images and the labeled information, a model can be trained based on the Machine Learning, which would be useful for generating new semantic information for the neighborhoods[12]. Timnit Gebru et al. proposed to estimate socio-economic information of US precincts based on massively collected geo-tagged street-level images[13]. GSV images were used to identify the make and model of parked cars in different neighborhoods. The identified car information was further used as predictors to estimate the political preference and the economic condition of the local residents. Based on time-series of GSV images, Nikhil Naik et al. measured the changes in the physical appearances of neighborhoods in five American cities[14]. The strong associations between the social characteristics and the streetscape changes show that the street-level images can help predict neighborhood improvement.

In this article, we presented our studies based on the street-level image analysis and a recently developed Deep Convolutional Neural Network (DCNN) to measure the spatial distributions of street greenery and the enclosure of street canyons. The results of this study highlight the potential of combining globally accessible GSV data with AI methods for urban studies.

1. 研究区域和谷歌街景地图数据收集流程。图1-1为在研究区域内选取的样本场地；图1-2为所收集的谷歌街景地图数据的元数据；图1-3为在6个不同水平方向上摄得的谷歌街景静态图；图1-4为其中一个场地的谷歌街景全景视图。

1. The study area and the workflow for GSV data collection. Figure 1-1 shows the created sample sites in the study area, Figure 1-2 is the collected metadata of GSV data, Figure 1-3 shows the static GSV images at six different horizontal directions, and Figure 1-4 is the GSV panorama of one site.

卫尔孝 © 1-1

Pano ID 街景编号	Longitude 经度	Latitude 纬度	Year 年份	Month 月份	Yaw 偏转角度
InaMj49WfB4t8BAde57eBW	-71.138718	42.399655	2007	08	265.268372
SRCvTTCdtOcHwy8klBwopw	-71.138658	42.39967	2011	12	266.387085
P-L4zZ/GxcRxw_XsmWW7Frw	-71.138656	42.399672	2012	01	266.983398
zJ7VBv6pFixr7nY8U2fJbQ	-71.138694	42.399666	2014	09	264.010559
y3Wr7AW4td7f_I7Fa3FV0A	-71.136078	42.399155	2007	08	358.268829
NRy5UDjBUh_lwQQQeRcT2Q	-71.136095	42.399143	2011	08	358.977631
P6sm7no8OOpPQRzwMHBp	-71.13609	42.399156	2012	01	359.18927
3ceXROggUgCQxe6lerol2Qs	-71.136099	42.399143	2013	09	359.33606
_M6XnP_D69coMmGalsnRB	-71.136095	42.399144	2014	09	359.063629
X44SILBzk8ob7LLAu3r32A	-71.136103	42.399154	2016	03	359.875671
G0NaLDLD0tSiyICJTn1Ulw	-71.135882	42.397507	2007	08	274.225098
731ebcCtYEP28kdnAa-QyA	-71.135884	42.397511	2011	08	275.571533
8KAVlhtKtXfdzuQ9jUxQPA	-71.135897	42.397512	2013	09	274.839783
dNbgUPQQKXEa8s-HtfBnZQ	-71.135886	42.397511	2014	09	274.432129
LKPWGb7-bkAqXgiXjN5zDw	-71.127241	42.396629	2007	08	140.692108
M6qNBuFHvPLhpMyz4ILmog	-71.127221	42.396618	2011	08	140.652771
Nr-peaQG5l3-kliolDilyg	-71.127232	42.396625	2013	09	141.104202
IIYOBdCHiKbJXGVULFBFXQ	-71.127235	42.396628	2014	09	140.779892
022VshHILHWJBZ2MvFsye9A	-71.127228	42.396623	2016	03	321.321777
VJStgPPGAjW8axV8HIdFXg	-71.128885	42.39623	2007	07	322.318146

卫尔孝 © 1-2

谷歌街景静态图应用程序接口
GSV Static Image API

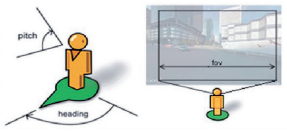

图片来源：谷歌地图
Source: Google Maps

© 李小江
1-3

© 李小江
1-4

研究中所使用的数据集包括街道地图与街道图像。街道地图由剑桥市政府授权使用，可用于收集街道图像。此外，我们主要采用在美国适用范围较广的谷歌街景地图进行研究。2007年，谷歌街景地图横空出世，与传统地图系统不同，其可以直接采集街道图像，并通过整合不同角度的街道图像创造出360° 的街道全景视图。

为利用谷歌街景地图收集静态图与全景视图，我们首先在研究区域范围内沿街道每隔100m设立一个样本场地。图1–1为在剑桥市沿街设立的样本场地示意图。在研究中，通过编写Python脚本，并输入每个样本场地的坐标，我们可进一步收集研究区域内的元数据与谷歌街景地图数据。此外，图1还依次展示了研究中谷歌街景地图中元数据（图1–2）、静态图（图1–3）和全景视图（图1–4）的收集流程。

3 利用深度学习网络实现图像分割

图像分割是从街道图像中获取空间信息的必要步骤。近来，由于基于深度学习的图像分割方法取得了较大进展，信息获取的准确性也大大提升。同时，开源数据库中大规模的图像数据集（如Cityscapes、

2 Study Area and Dataset

In this study, we chose City of Cambridge, Massachusetts as the study area. Located directly north of Boston across Charles River, Cambridge is the fifth most populous city in the state of Massachusetts, with a total population of 105,000.

The dataset used in this study includes street map and street-level images. The street map accessed from the city government was used to collect the street-level images. Since GSV has a dense coverage in the United States, we used GSV images in this study. GSV was launched in 2007 and differentiates itself from traditional mapping system by directly capturing the visual appearance of streetscapes. By stitching the images taken in different angles together, GSV can create a continuous 360° panorama of a streetscape.

In order to collect GSV static images and panoramas, we first created sample sites every 100 m along the streets in the study area. Figure 1-1 shows the generated sample sites along streets in Cambridge. In this study, by developing a Python script and using the coordinates of sample sites as the input, we further collected the metadata and GSV data in the study area. Figure 1 shows the workflow for collecting GSV metadata (Fig. 1-2), static GSV images (Fig. 1-3), and the GSV panoramas (Fig. 1-4).

3 Deep Learning Network for Image Segmentation

The image segmentation is a requisite step to derive spatial information from street-level images. Recent progress in Deep-Learning-based methods enables researchers to extract information more accurately. Concurrently, the availability of large-scale and open-source image datasets, such as Cityscapes dataset, Mapillary Vistas, and ADE20K, provides researchers with sufficient data to train Deep-Learning-based

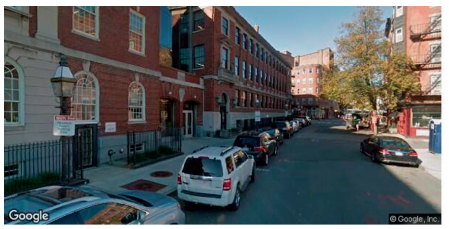

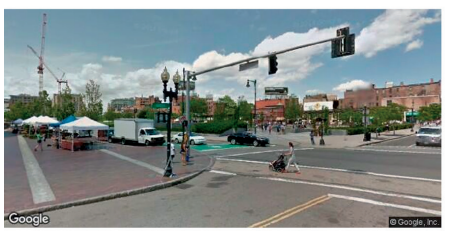

谷歌街景静态图
Static GSV images

图像分割结果
Image segmentation results

图1 谷歌街景静态图及图像分割结果
2-1

谷歌街景全景视图
GSV panoramas

图像分割结果
Image segmentation results

图2 谷歌街景全景视图及图像分割结果
2-2

Mapillary Vistas和ADE20K等平台）为研究者提供了充足的数据，可对基于深度学习的模型进行训练，使其准确识别图片特征。

在本项研究中，我们采用的是DCNN的其中一种——金字塔场景解析网络（PSPNet），经过在ADE20K数据集中的训练[15]，其可实现对谷歌街景静态图和全景视图的分割。PSPNet使用一种全新的神经网络子结构，通过对前期的卷积层输出结果进行多尺度的呈现，保留全局与局部的背景信息。PSPNet对于ADE20K数据集中复杂视觉场景的分割极为先进，能够达到像素级的精度。因此，基于PSPNet在ADE20K数据集训练过程中稳定的良好表现，我们更加确信其能够准确分割图像中未受建筑物、树木和其他环境因素遮挡的天空区域。图2展示了PSPNet对作为样本的谷歌街景静态图和全景视图进行图像分割的结果。

4 街道绿地测量与绘制

因与人类在地面观察的视角更为贴近，街道图像提供了一种测量街道绿地的新角度。在本项研究中，我们利用改进后的绿色视觉指数

models to accurately identify features in images.

In this study, we applied the Pyramid Scene Parsing Network (PSPNet), a DCNN trained on the ADE20K dataset[15] to segment the static GSV images and panoramas. The PSPNet uses a new neural network sub-architecture, which retains global and local contextual information through a multi-scale representation of the previous convolutional layer's output. The PSPNet achieved the state-of-the-art performance in pixel-level segmentation of complex visual scenes in the ADE20K dataset. Hence, the validated performance of the PSPNet trained on the ADE20K dataset makes us confident to use the PSPNet to accurately segment areas of the sky that are unobstructed by buildings, trees, and other environmental factors. Figure 2 shows the image segmentation results of sample GSV images and panoramas using the PSPNet.

4 Measuring and Mapping the Street Greenery

Using the street-level images helps us measure the street greenery from a ground viewing angle. In this study, we used the modified Green View Index (GVI) to quantify the street greenery[10]. The GVI was defined as the percentage of the total

2. 经过图像分割后的谷歌街景静态图（图2-1）和利用PSPNet分割后的谷歌街景全景视图（图2-2）。
3. 利用谷歌街景地图，在其中一个样本场地中选取6个不同水平方向所摄图像。
4. 马萨诸塞州剑桥市GVI的空间分布情况。

2. Image segmentation results on static GSV images (Fig. 2-1) and GSV panoramas using PSPNet (Fig. 2-2).
3. GSV images captured in six different horizontal directions at one sample site.
4. The spatial distribution of GVI in Cambridge, Massachusetts.

（GVI）来对街道绿地进行量化分析[10]。GVI即在同一场地拍摄的不同视角的6张图片中出现的绿色像素数量之和占6张图片总像素数量的百分比，其计算公式如下：

$$GVI = \frac{\sum_{i=1}^{6} 区域_{g\_i}}{\sum_{i=1}^{6} 区域_{t\_i}} \times 100\%$$

图3中的6张图片分别拍摄于同一场地水平方向的6种不同角度(0°、60°、120°、180°、240°和300°)，公式中区域$_{g_i}$为第i种角度的图片中绿色像素的数量，区域$_{t_i}$为第i种角度的图片中全部像素数量之和。这6张图片对同一地点水平方向的景象实现了360°全覆盖，以计算街道中每个样本场地的GVI。在本研究中，我们主要利用经过深度学习训练之后的模型来计算分割后的谷歌街景静态图中绿色像素的数量，而GVI则反映了人们在街道中所能看到的绿色景观的多少。

图4为剑桥市不同区域的GVI分布图，GVI平均值为25.59。从图中可见，其GVI在空间分布上呈现出较为明显的特征，概括而言即研究区域的西部与西北部相比东部拥有更多的绿地。

green pixels from six images taken at a same site to the total pixel numbers of the six images, calculated using the following formula,

$$GVI = \frac{\sum_{i=1}^{6} Area_{g\_i}}{\sum_{i=1}^{6} Area_{t\_i}} \times 100\%$$

where Area$_{g_i}$ is the number of green pixels in the image taken in the ith direction among the six different horizontal directions (0°, 60°, 120°, 180°, 240°, and 300°) for one site (Fig. 3), and Area$_{t_i}$ is the total pixel number of the image taken in the ith direction. The six images cover 360° horizontal surroundings to calculate the index for each sample site along streets. In this study, the number of green pixels in the image can be calculated by the trained Deep Learning model based on the segmented static GSV images. The GVI represents how much greenery people can see on the ground based on the street-level images.

Figure 4 shows the spatial distribution of the GVI in Cambridge, and the mean GVI value is 25.59. There is a clear overall pattern of the spatial distribution of the GVI in Cambridge: the western and northwestern parts of the study area are greener than the eastern part.

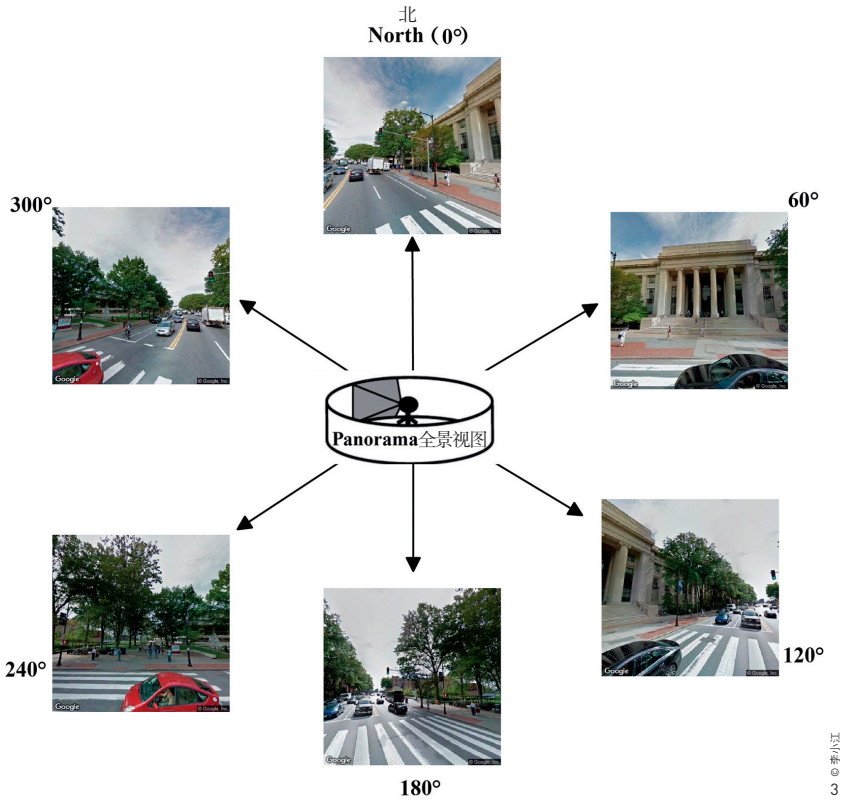

王小李 © 3

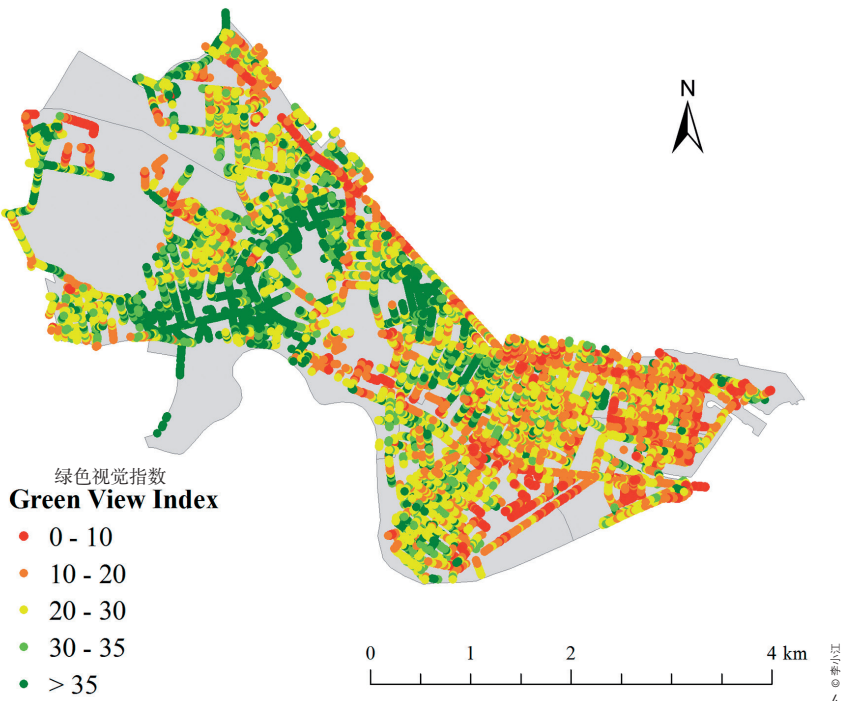

王小李 © 4

在谷歌街景静态图应用程序接口的帮助下，我们可利用开放的谷歌街景地图收集任何一处场地的街道图像[10]，进而自动计算出场地GVI。研究中所选取的样本场地均匀地分布于住宅区街道中，因而基于街道图像计算的GVI能够更好地反映城市街道的绿地量。由此生成的GVI地图则可进一步用于城市树木管理与公共健康研究。

5 街道峡谷围合度估测与绘制

作为衡量城市几何结构的无量纲参数，城市天空开阔度（SVF）是对街道峡谷的开阔程度进行几何量化分析的重要指标[16]~[19]，它反映了天空所受遮挡的程度[20]~[22]。SVF是平面地面所受辐射与整个视域半球所受辐射的比例[23]。其计算公式如下[24]：

$$\mathrm{SVF} = \frac{1}{\pi r_0^2}\int_{S^p} dS^p$$

其中r_0为半球辐射环境的半径，S^p为圆形天空投射在地面上的面积。若天空完全受到遮挡，SVF为0；若天空完全不受遮挡，则SVF为1。

目前，SVF已被应用于林地、城市气候、城市化、空气污染及城市热岛效应等相关研究中[7][22][25]~[32]。基于半球图像的摄影法是估算SVF的标准方法之一，而谷歌街景全景视图的发展则为大规模自动生成半球

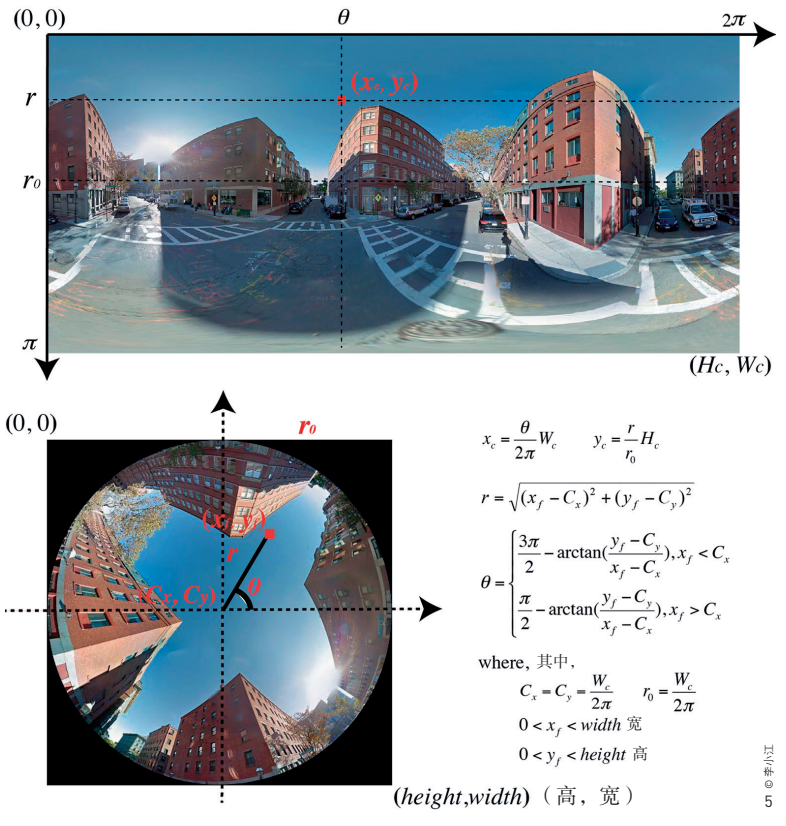

5

By using the GSV Static Image Application Programming Interface, street-level images can be collected for any site with GSV image available[10]. This allows the street-level image based GVI to be calculated for any site with street-level images available automatically. In this study, the sample sites are located evenly along residential streets, which make the street-level image based GVI better to represent the street greenery in cities. The GVI map can be used for urban tree management and public health studies.

5 Estimating and Mapping the Enclosure of Street Canyons

As a dimensionless parameter of urban geometry, the Sky View Factor (SVF) is an important geometric quantification of the openness of street canyons[16]~[19]. The SVF indicates how much sky is obstructed[20]~[22], and also represents the ratio between radiation received by a planar ground and that from the entire hemisphere's input radiation[23]. The SVF is defined as[24]:

$$\mathrm{SVF} = \frac{1}{\pi r_0^2}\int_{S^p} dS^p$$

where r_0 is the radius of the hemispheric radiating environment, S^p is the area of the circle sky area projected on the ground. When the sky is totally obstructed, the SVF is zero; while the SVF is one when there is no obstruction at all.

The SVF has been applied in studies of forestry, urban climate, urbanization, air pollution, and urban heat island effects[7][22][25]~[32]. The photographic method based on hemispherical images is one of the standard methods for estimating SVF. GSV panoramas provide a new data source for generating hemispherical images and estimating SVF at a large-scale automatically. Figure 2-2 shows the collected GSV panoramas in the form of equidistant cylindrical projection. For SVF estimation, the cylindrical GSV panoramas need to be transformed to equidistant azimuthal projection. Figure 5 shows the geometric model of transforming cylindrical projection to azimuthal projection[19]. A GSV panorama with width of W_c and height of H_c can be re-projected to an azimuthal hemispherical image with the width and height of W_c/π.

Figure 6 shows the image segmentation results of the GSV panoramas and the generated hemispherical images based on the geometrical model. Based on the segmentation results of the hemispherical images, the SVF can be calculated with the standard photographic method[24][33], which first divides

5. 将等距圆柱投影转换为等距方位投影（半球图像）的几何变换过程。
6. 谷歌街景全景视图的分割结果可用于估算SVF。(a)为全景视图的分割结果，(b)为半球图像的分割结果。
7. 马萨诸塞州剑桥市SVF的空间分布情况。

5. Geometrical transform of equidistant cylindrical projection to equidistant azimuthal projection (hemispherical image).
6. The GSV panorama segmentation results used for SVF estimation. Section (a) shows the segmentation results of GSV panoramas, and section (b) shows the segmentation results of hemispherical images.
7. The spatial distributions of SVF in Cambridge, Massachusetts.

图像并估算SVF提供了全新的数据来源。图2–2展示了以等距圆柱投影方式收集到的谷歌街景全景视图。为估算SVF，圆柱状的谷歌街景全景视图需转换为等距方位投影。图5即为将圆柱投影转换为方位投影的几何模型示意图[19]。宽度为W_c、高度为H_c的谷歌街景全景视图可被重新投影为宽和高均为W_c/π的方位半球图像。

图6展示了基于几何模型生成的谷歌街景全景视图及半球图像的图像分割结果。基于半球图像的图像分割结果，我们可以通过标准摄影法计算得出SVF。此处所采用的摄影法[24][33]即首先将鱼眼图像分为n个等宽的同心圆环，而后计算所有代表未被遮挡的天空的环形部分之和。此处的SVF计算公式如下：

$$SVF = \frac{1}{2\pi}\sin\left(\frac{\pi}{2n}\right)\sum_{i=1}^{n}\sin\left(\frac{\pi(2i\text{-}1)}{2n}\right)\alpha_i$$

其中n是所有圆环的个数之和，i是圆环指数，α_i是第i个圆环的角宽。

图7呈现了基于谷歌街景的摄影法计算得出的SVF的空间分布情况，其数值反映了夏季街谷的开阔程度。由于研究中所采用的谷歌街景全景视图拍摄于树木枝繁叶茂的季节，建筑物与行道树均对街谷中的太阳辐射起到了一定的遮挡作用，因此SVF分布图所呈现的规律不如GVI分布图（图4）清晰明了。对比图7与图4可见，在GVI较大的区域，

the fisheye image into several concentric annular rings of equal width, and then sums up all annular sections representing the visible sky. The SVF is then calculated as,

$$SVF = \frac{1}{2\pi}\sin\left(\frac{\pi}{2n}\right)\sum_{i=1}^{n}\sin\left(\frac{\pi(2i\text{-}1)}{2n}\right)\alpha_i$$

where n is the total number of rings, i is the ring index, and α_i is the angular width in ith ring.

Using the GSV-based photographic method, Figure 7 shows the spatial distribution of the estimated SVF values, which represent the openness of street canyons in summer. Since GSV panoramas used in this study were captured during leaf-on seasons, therefore, building blocks and street trees both act as obstructions of solar radiation in street canyons. Thus, the

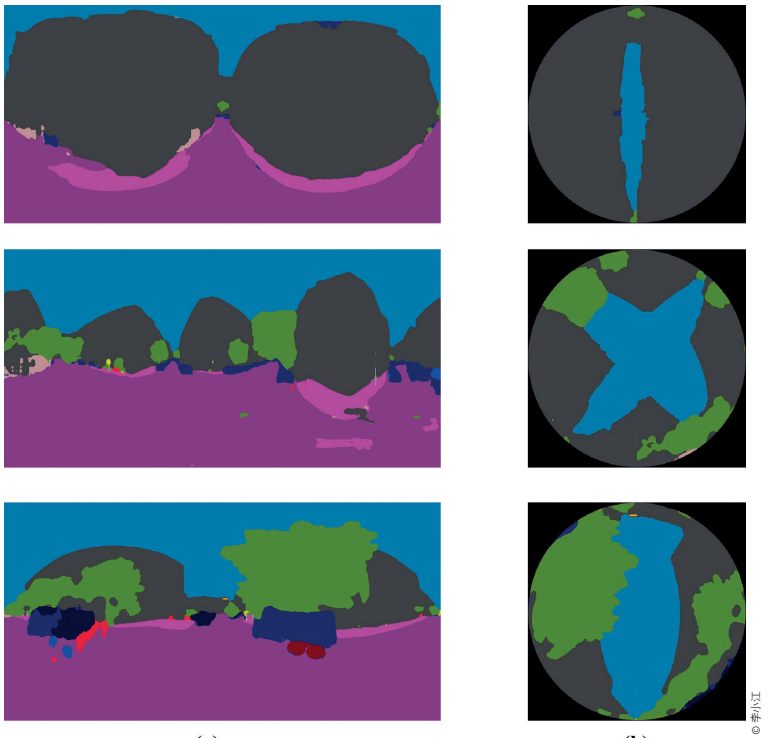

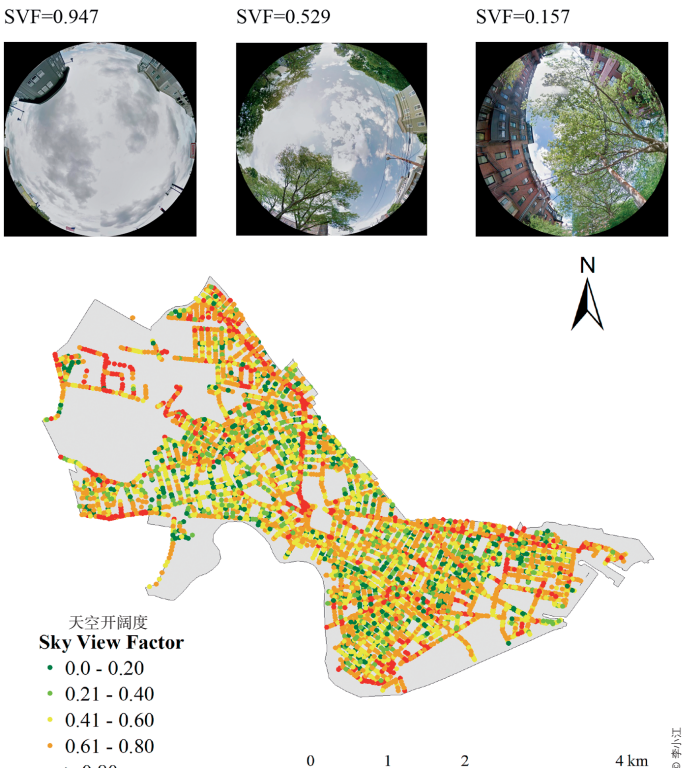

SVF往往偏小，这是由于街道绿地通常环绕于街谷周边，降低了SVF的数值。此外，如果场地内高层建筑物较多，该区域的SVF相对其他区域也较低。以坐落于研究区域东南部的肯德尔广场为例，其SVF便低于其他区域。

6 讨论与结论

本项研究利用开源街道图像，呈现了最新开发的深度学习算法在剑桥市城市景观分析中的两项应用。由于侧面视角的街道图像与人们在地面的视角相似，因此可更好地反映人们对环境的体验。基于谷歌街景地图所提供的量化信息，我们进一步测绘出了剑桥市的街道绿地量与城市街谷的开阔程度。这些从街道图像中估算而得的数值能够为城市规划师、公共健康研究员及社会科学家等提供全新的视角，以更好地研究人类与自然环境之间的互动关系。除谷歌街景地图外，腾讯、微软、百度及Mapillary等同类企业均相继推出了街景地图功能，其所提供的街道图像在分辨率与覆盖范围方面均在不断提升。新兴的无人驾驶技术也将为未来的城市研究提供更丰富的街道图像。对于不便采用数字城市模型和高空间分辨率遥感数据的研究区域，街道图像提供了适宜的替代方案。因此，城市环境研究将大大受益于当前和未来的街道图像发展。

随着人工智能的不断发展，我们能够从街道图像中提取更为高级的信息，这在以往是难以实现的。DCNN亦可帮助准确识别街道中的不同城市特征（图2）。而根据图像分割的结果，我们可以准确地估算出街道绿地量和街谷开阔程度。此外，适用于大规模系统的深度学习工具更是大大提高了研究的自动化水平，而不再需要过多的人为干预。因此，本研究所采用的方法可被大量应用于城市研究之中。通过基于

spatial pattern of the SVF distribution is not as clear as the GVI map (Fig. 4). Compared with the GVI map, those sites with larger GVI values usually have lower SVF values. This is because the existence of the street greenery would enclose the street canyons and lead to lower SVF values. In addition, for those sites located in areas with a lot of high-rise buildings, the SVF values are much lower than other sites. For instance, in Kendal Square located in southeastern part of the study area, the SVF values are lower than that of other sites.

6 Discussion and Conclusion

This study presented two applications of recently developed Deep Learning algorithm on landscape analysis in Cambridge using publicly accessible street-level images. The profile view street-level images share a similar perspective with people on the ground, and can be used to map the human-scale natural experience. Based on the quantitative information derived from GSV images, we further estimated and mapped the visibility of street greenery and the openness of street canyons in Cambridge. These metrics of city streets derived from street-level images would help urban planners, public health researchers, and social scientists to investigate the interaction of physical environment and human beings from a new perspective at a fine level. Other than GSV, street-level images are increasing in resolution and coverage through competing providers, such as Tencent Street View, Microsoft Streetside, Baidu Street View, and Mapillary. Emerging autonomous vehicle technologies would also provide more abundant street-level images for urban studies in future. Street-level images are good substitutes for study areas where digital city models and high spatial resolution remotely sensed data are not available. Therefore, urban environmental studies can benefit significantly from the current and future state of street-level imagery.

The recent progress in AI makes it possible to extract high-level information from street-level images that previously was not possible. Different kinds of the urban features along the streets can be recognized accurately (Fig. 2) using DCNN. Based on the image segmentation results, we can accurately estimate the extent of street greenery and openness of street canyons. Furthermore, the ability of Deep Learning tools to fit into large-scale systems allows us to build this study's workflow in a fully automatic manner that does not require human intervention. Therefore, the method used in this study can be applied at a large-scale for urban studies. Based on the SVF map and the hemispherical images generated from street-

街道图像而绘制的SVF分布图和半球图像，我们可以了解各时段太阳辐射的空间分布情况，并估算地面接收到的太阳辐射。本研究所提出的方法能够帮助研究人员、城市规划师和城市管理者更好地理解街道景观对未来公众健康、城市微气候及人们对于城市环境感知的影响。

本项研究基于街道图像，展示了人工智能的最新发展成果在城市景观分析中的具体应用，并展望了其在未来可能的应用模式，例如，我们可以探究街道景观的年变化或季节性变化对人们日常体验的影响。在此类研究中，深度学习工具可帮助定量描述时间更迭对城市绿地的影响。**LAF**

level images, it is possible to estimate the spatial distribution of the sunlight duration and how much solar radiation is reaching the ground. The method proposed in this study can help researchers, urban planners, and managers have a better understanding of the influence of streetscapes on the public health, urban microclimate, and human perception of urban environment in future.

In this study, we present specific applications of the recent progress in AI in urban landscape studies based on street-level images, with an awareness of the potential for future applications. Such applications can be used for studying annual and seasonal changes of streetscapes and their impacts on human daily experiences, while utilizing Deep Learning tools to quantify changes in urban greenery due to changes of time. **LAF**

REFERENCES

[1] Li, X. J., Ratti, C., & Seiferling, I. (2017, July). Mapping Urban Landscapes along Streets Using Google Street View. In M. Peterson (Ed.), Advances in Cartography and GIScience, ICACI 2017, Lecture Notes in Geoinformation and Cartography in International Cartographic Conference (pp. 341-356). Cham: Springer.

[2] Camacho-Cervantes, M., Schondube, J. E., Castillo, A., & MacGregor-Fors, I. (2014). How do people perceive urban trees? Assessing likes and dislikes in relation to the trees of a city. Urban Ecosystems, 17(3), 761-773.

[3] Balram, S., & Dragićević, S. (2005). Attitudes toward urban green spaces: integrating questionnaire survey and collaborative GIS techniques to improve attitude measurements. Landscape and Urban Planning, 71(2-4), 147-162.

[4] Schroeder, H. W., & Cannon, W. N. (1983). The esthetic contribution of trees to residential streets in Ohio towns. Journal of Arboriculture, 9(9), 237-243.

[5] Ulrich, R. (1984). View through a window may influence recovery. Science, 224(4647), 420-421.

[6] Pazhouhanfar, M., & Kamal, M. (2014). Effect of predictors of visual preference as characteristics of urban natural landscapes in increasing perceived restorative potential. Urban Forestry and Urban Greening, 13(1), 145-151.

[7] Carrasco-Hernandez, R., Smedley, A. R., & Webb, A. R. (2015). Using urban canyon geometries obtained from Google Street View for atmospheric studies: Potential applications in the calculation of street level total shortwave irradiances. Energy and Buildings, (86), 340-348.

[8] Asgarzadeh, M., Lusk, A., Koga, T., & Hirate, K. (2012). Measuring oppressiveness of streetscapes. Landscape and Urban Planning, 107(1), 1-11.

[9] Asgarzadeh, M., Koga, T., Hirate, K., Farvid, M., & Lusk, A. (2014). Investigating oppressiveness and spaciousness in relation to building, trees, sky and ground surface: A study in Tokyo. Landscape and Urban Planning, (131), 36-41.

[10] Li, X., Zhang, C., Li, W., Ricard, R., Meng, Q., & Zhang, W. (2015). Assessing street-level urban greenery using Google Street View and a modified green view index. Urban Forestry and Urban Greening, 14(3), 675-685.

[11] Salesses, P., Schechtner, K., & Hidalgo, C. A. (2013). The collaborative image of the city: mapping the inequality of urban perception. PloS ONE, 8(7), e68400.

[12] Naik, N., Philipoom, J., Raskar, R., & Hidalgo, C. (2014, June). Streetscore predicting the perceived safety of one million streetscapes. In Proceedings of the IEEE Conference on Computer Vision and Pattern Recognition Workshops (pp. 793-799). IEEE Computer Society, Washington.

[13] Gebru, T., Krause, J., Wang, Y., Chen, D., Deng, J., Aiden, E. L., & Li, F. F. (2017). Using deep learning and Google Street View to estimate the demographic makeup of the US. Proceedings of the National Academy of Sciences, 114(50), 13108-13113.

[14] Naik, N., Kominers, S. D., Raskar, R., Glaeser, E. L., & Hidalgo, C. A. (2017). Computer vision uncovers predictors of physical urban change. Proceedings of the National Academy of Sciences, 114(29), 7571-7576.

[15] Zhao, H., Shi, J., Qi, X., Wang, X., & Jia, J. (2017, July). Pyramid scene parsing network. In IEEE Conference on Computer Vision and Pattern Recognition (pp. 6230-6239). IEEE Computer Society, Honolulu.

[16] Oke, T. R. (1981). Canyon geometry and the nocturnal urban heat island: Comparison of scale model and field observations. Journal of Climatology, 1(3), 237-254.

[17] Chapman, L., & Thornes, J. E. (2004). Real-time sky-view factor calculation and approximation. Journal of Atmospheric and Oceanic Technology, 21(5), 730-741.

[18] Ratti, C., & Richens, P. (2004). Raster analysis of urban form. Environment and Planning B: Planning and Design, 31(2), 297-309.

[19] Li, X., Ratti, C., & Seiferling, I. (2018). Quantifying the shade provision of street trees in urban landscape: A case study in Boston, USA, using Google Street View. Landscape and Urban Planning, (169), 81-91.

[20] Hwang, R. L., Lin, T. P., & Matzarakis, A. (2011). Seasonal effects of urban street shading on long-term outdoor thermal comfort. Building and Environment, 46(4), 863-870.

[21] Lee, H., Holst, J., & Mayer, H. (2013). Modification of human-biometeorologically significant radiant flux densities by shading as local method to mitigate heat stress in summer within urban street canyons. Advances in Meteorology, (38), 1-13.

[22] Lin, T. P., Tsai, K. T., Hwang, R. L., & Matzarakis, A. (2012). Quantification of the effect of thermal indices and sky view factor on park attendance. Landscape and Urban Planning, 107(2), 137-146.

[23] Watson, I. D., & Johnson, G. T. (1987). Graphical estimation of sky view-factors in urban environments. International Journal of Climatology, 7(2), 193-197.

[24] Steyn, D. G. (1980). The calculation of view factors from fisheye lens photographs. Atmosphere-Ocean, 18(3), 254-258.

[25] Holmer, B., Postgård, U., & Eriksson, M. (2001). Sky view factors in forest canopies calculated with IDRISI. Theoretical and Applied Climatology, 68(1-2), 33-40.

[26] Grimmond, C. S. B., Potter, S. K., Zutter, H. N., & Souch, C. (2001). Rapid methods to estimate sky-view factors applied to urban areas. International Journal of Climatology, 21(7), 903-913.

[27] Debbage, N. (2013). Sky-view factor estimation: A case study of Athens, Georgia. The Geographical Bulletin, 54(1), 49-57.

[28] Hämmerle, M., Gál, T., Unger, J., & Matzarakis, A. (2011). Comparison of models calculating the sky view factor used for urban climate investigations. Theoretical and Applied Climatology, 105(3-4), 521-527.

[29] Unger, J. (2009). Connection between urban heat island and sky view factor approximated by a software tool on a 3D urban database. International Journal of Environment and Pollution, 36(1-3), 59-80.

[30] Eeftens, M., Beekhuizen, J., Beelen, R., Wang, M., Vermeulen, R., Brunekreef, B., Huss, A., & Hoek, G. (2013). Quantifying urban street configuration for improvements in air pollution models. Atmospheric Environment, (72), 1-9.

[31] Chen, L., Ng, E., An, X., Ren, C., Lee, M., Wang, U., & He, Z. (2012). Sky view factor analysis of street canyons and its implications for daytime intra-urban air temperature differentials in high-rise, high-density urban areas of Hong Kong: a GIS-based simulation approach. International Journal of Climatology, 32(1), 121-136.

[32] Svensson, M. K. (2004). Sky view factor analysis — implications for urban air temperature differences. Meteorological Applications, 11(3), 201-211.

[33] Johnson, G. T., & Watson, I. D. (1984). The determination of view-factors in urban canyons. Journal of Climate and Applied Meteorology, 23(2), 329-335.